Chemical Research in Toxicology

pubs.acs.org/crt

Article

Role of UDP-Glycosyltransferase (*ugt*) Genes in Detoxification and Glycosylation of 1-Hydroxyphenazine (1-HP) in *Caenorhabditis elegans*

Muhammad Zaka Asif, Kelsey A. Nocilla, Li Ngo, Man Shah, Yosef Smadi, Zaki Hafeez, Michael Parnes, Allie Manson, John N. Glushka, Franklin E. Leach, III, and Arthur S. Edison*

Cite This: *Chem. Res. Toxicol.* 2024, 37, 590−599

Read Online

ACCESS | Metrics & More | Article Recommendations | Supporting Information

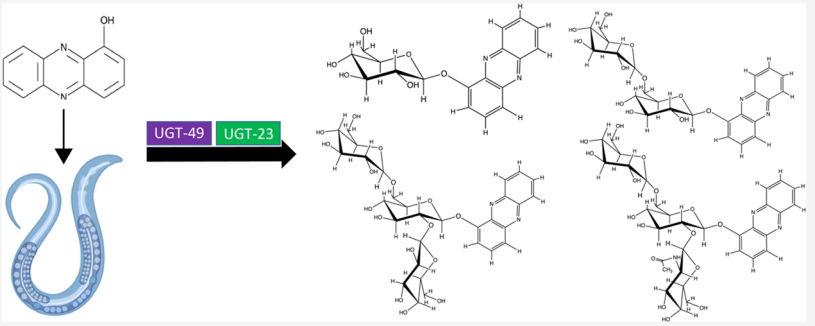

ABSTRACT: *Caenorhabditis elegans* is a useful model organism to study the xenobiotic detoxification pathways of various natural and synthetic toxins, but the mechanisms of phase II detoxification are understudied. 1-Hydroxyphenazine (1-HP), a toxin produced by the bacterium *Pseudomonas aeruginosa*, kills *C. elegans*. We previously showed that *C. elegans* detoxifies 1-HP by adding one, two, or three glucose molecules in N2 worms. Our current study evaluates the roles that some UDP-glycosyltransferase (*ugt*) genes play in 1-HP detoxification. We show that *ugt-23* and *ugt-49* knockout mutants are more sensitive to 1-HP than reference strains N2 or PD1074. Our data also show that *ugt-23* knockout mutants produce reduced amounts of the trisaccharide sugars, while the *ugt-49* knockout mutants produce reduced amounts of all 1-HP derivatives except for the glucopyranosyl product compared to the reference strains. We characterized the structure of the trisaccharide sugar phenazines made by *C. elegans* and showed that one of the sugar modifications contains an *N*-acetylglucosamine (GlcNAc) in place of glucose. This implies broad specificity regarding UGT function and the role of genes other than *ogt-1* in adding GlcNAc, at least in small-molecule detoxification.

INTRODUCTION

Caenorhabditis elegans are bacterivores found in soil and decaying organic matter.[1] As they feed on bacteria in their environment, they are exposed to numerous pathogens and xenobiotics.[2] To combat exposure, worms have developed three main strategies for defense. One is avoidance, where they can sense potentially hostile environments and avoid going to them.[3] Another is the presence of a strong cuticle and pharyngeal grinder to physically prevent pathogens from entering the worm.[4] Finally, if pathogens can enter the worm, several mechanisms are activated, constituting the innate immune response.

Along with the pathogen response, the *C. elegans* innate immune system is activated upon xenobiotic exposure. Xenobiotics are defined as substances foreign to a body or ecological system. In nature, *C. elegans* feed on various bacteria, many of which produce compounds that are toxic to the worms. As a result, *C. elegans* has developed a wide array of detoxification enzymes.[5] Xenobiotic metabolism is canonically divided into three phases.[6] Phase I is the addition of reactive moieties such as hydroxyl groups to the parent xenobiotic. Phase II is the conjugation of either the phase I modified xenobiotic or parent xenobiotic to a water-soluble molecule to facilitate excretion. Phase III is the transport of these metabolized compounds out of the cell.[7] In this study, we focus on steps involved in the phase II detoxification of one such xenobiotic: 1-hydroxyphenazine (1-HP).

1-Hydroxyphenazine (1-HP) is a small molecule produced by many Pseudomonas species, including *Pseudomonas aeruginosa*, a Gram-negative bacterium that causes disease in higher eukaryotes such as humans.[8,9] In humans, 1-HP is

Received: December 19, 2023
Revised: February 26, 2024
Accepted: February 27, 2024
Published: March 15, 2024

known to affect ciliary function, especially in patients with cystic fibrosis.[9] 1-HP is one of three related metabolites, along with pyocyanin and phenazine-1-carboxylic acid, produced by *P. aeruginosa* that are toxic to *C. elegans*.[10] 1-HP is thought to cause chronic toxicity in *C. elegans* by generating α-synuclein- and polyglutamine-induced protein misfolding and exacerbating α-synuclein-induced dopaminergic neurodegeneration.[11] *C. elegans* modifies 1-HP by adding one, two, or three glucose moieties, with phosphorylation also observed in the endometabolome.[12] In this study, we sought to more thoroughly characterize the metabolized 1-HP derivatives produced by *C. elegans* and to conduct preliminary experiments on the *ugt* gene family, which is likely involved in at least some of these modifications.

UGTs are a family of enzymes critical for the homeostatic regulation of endogenous metabolites and xenobiotic detoxification in several organisms, including humans and *C. elegans*.[13] While humans only have 22 *ugt* genes, *C. elegans* have over 70.[14,15] Not all *C. elegans ugt* genes have obvious human homologues, but they do have homologues in parasitic nematodes, making them potential targets to combat anthelmintic resistance.[16] UGTs are the primary protein family responsible for adding glucose moieties during phase II xenobiotic detoxification in *C. elegans*.[7] Loss or modification of UGTs has been implicated in drug hypersensitivity.[16,17] They have also been shown to be upregulated upon exposure to metals, pathogenic toxins, anthelmintics, and other small molecules.[16,18]

RESULTS AND DISCUSSION

Quantitation of 1-HP Derivatization in *ugt* Mutants. In this study, we tested available *ugt* mutants for their involvement in 1-HP modification and susceptibility (Table 1, Supporting Information Table 1). We analyzed the phylogeny of these *ugt* genes and found that they covered most of the clades in the UGT family[15] (Supporting Information Figure 1). We then adapted a plate-based mortality screen from our previous work to discover strains with modified sensitivity to 1-HP exposure at the LD_{50} (179 μM) concentration (Figure 1A).[23] All strains were paired with N2, and PD1074 replicates were used as reference controls. PD1074 is 99.98% identical to N2 and is currently recommended as the new reference *C. elegans* strain because N2 has significantly diverged over time and is no longer a reliable reference.[21] We found that all strains had higher mortality when exposed to 179 μM 1-HP than the bacteria control. The solvent, 1.1% dimethyl sulfoxide (DMSO), sometimes trended to higher mortality, but this was not statistically significant after performing a one-way analysis of variance (ANOVA) for each strain (Supporting Information Figure 2B).

Table 1. Information on Strains Used in This Study[a]

strain name	genotype	refs	time from egg to L4 (h)
N2		[b]	~42
PD1074		[c]	~42
RB2055	*ugt-1*	[d]	~44
VC4207	*ugt-6*	[e]	~42
VC3950	*ugt-9*		~42
RB2550	*ugt-23*	[d]	~42
PH7346	*ugt-23*	[g]	~42
RB2607	*ugt-49*	[d]	~44
VC2512	*ugt-60*	[f]	~50
RB2011	*ugt-62*	[d]	~46
VC4339	*ugt-66*	[e]	~42
RB1342	*ogt-1*[h]	[d]	~43

[a]All strains except PH7346 were obtained from the Caenorhabditis Genetics Center (CGC). [b]Ref 19. The genetics of *C. elegans* (domesticated laboratory strain of *C. elegans*) (obtained via CaeNDR).[20] [c]Ref 21. Recompleting the *C. elegans* genome (a newer standardized version of the laboratory strain of *C. elegans*) (obtained via CaeNDR).[20] [d]Ref 22. *C. elegans* Gene Knockout Project at the Oklahoma Medical Research Foundation. [e]CRISPR/Cas9 Methodology for the Generation of Knockout Deletions in *C. elegans*. [f]*C. elegans* Reverse Genetics Core Facility at the University of British Columbia, International *C. elegans* Gene Knockout Consortium. [g]SUNY Biotech. [h]Note: *ogt-1* is included in this table as this strain was used for toxicity experiments as well based on results described in Figure 2.

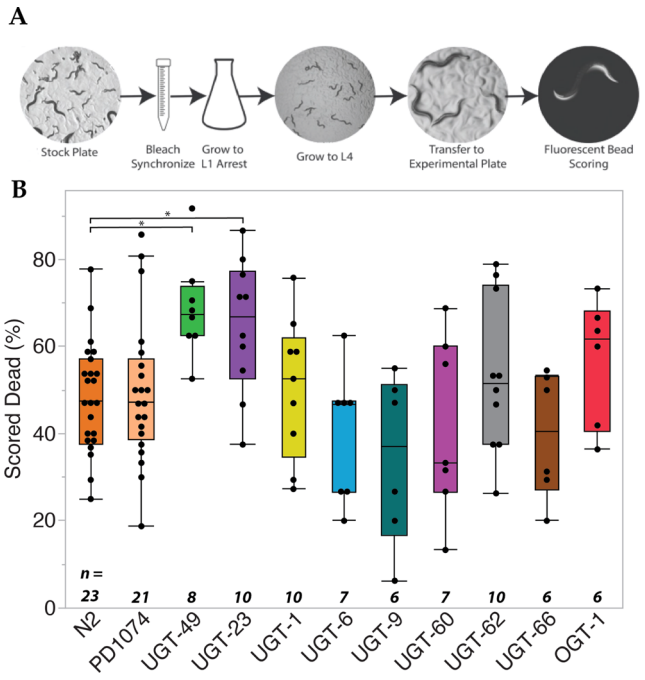

Figure 1. Plate-based screen for the susceptibility to 1-HP. (A) Schematic describing the method for the plate-based assay. Worms were incubated for 7 h with at least six replicates per strain. (B) Box and whisker plot with quartiles showing mortality of various strains at 179 μM 1-HP. Horizontal lines with * indicate significantly ($P < 0.1$) increased mortality compared to N2 with an α of 0.1 after a Wilcoxon pairwise comparison, followed by a Benjamini–Hochberg Correction. The number of replicates (n) for each strain is provided below each plot.

We tested 11 different strains for 1-HP exposure (Table 1). Of these strains, N2 and PD1074 had already been tested in previous studies.[12,23] In our assay, N2 worms had a mean mortality of 48.2% with a standard error of 2.6 ($n = 23$), while PD1074 had a mean of 49.5% with a standard error of 2.7 ($n = 21$). We performed a one-way ANOVA in both cases, suggesting that the mortality by 1-HP exposure was significantly greater than in both the bacteria-only and DMSO controls ($P < 0.0001$) (Supporting Information Figure 2A). In the other strains we tested (Table 1, Supporting Information Table 1), we found that all of the strains except *ugt-23* and *ugt-49* had a mortality percentage between 35 and 54% compared to controls ($P < 0.01$) (Supporting Information

https://doi.org/10.1021/acs.chemrestox.3c00410
Chem. Res. Toxicol. 2024, 37, 590−599

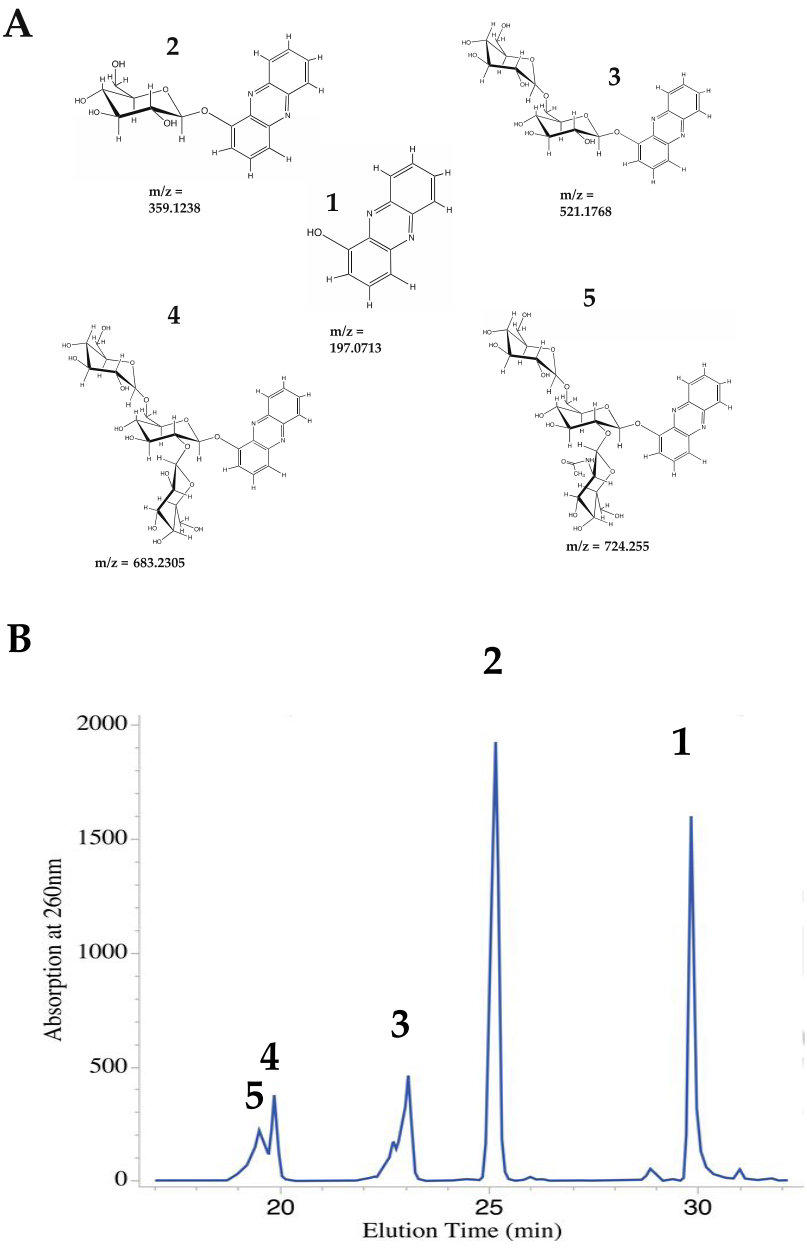

Figure 2. Compounds detected during the analysis of the culture supernatant from PD1074 exposed to 1-HP. (A) 1-HP and its glycosylated derivatives with their corresponding *m*/*z* values. (**1**) 1-HP, (**2**) *β*-D-glucopyranosyl-phenazine, (**3**) *β*-D-glucopyranosyl (1−6)-*β*-D-glucopyranosyl-phenazine, (**4**) *β*-D-glucopyranosyl (1−6)- [*β*-D-glucopyranosyl (1−2)]-*β*-D-glucopyranosyl-phenazine, and (**5**) *β*-D-glucopyranosyl (1−6)-[*β*-D-*N*-acetylglucosamine-pyranose (1−2)]-*β*-D-glucopyranosyl-phenazine. The *m*/*z* values were obtained from high-resolution MS data acquired using positive-ion electrospray ionization (ESI) (Supporting Information Table 2). (B) Representative UV chromatogram of PD1074 exposed to 22.3 *μ*M 1-HP for 24 h in an S-basal medium with 2% *Escherichia coli*. Each peak corresponds to either 1-HP or one of its glycosylated derivatives. The peak at 30 min is (**1**), the peak at 25 min is (**2**), the peak at 23 min is (**3**), the peak at 19.8 min is (**4**), and the peak at 19.4 min is (**5**).

Figure 2A). The strain *ugt-23* had a mortality of 64.7% with a standard error of 3.7 (n = 10), and *ugt-49* had a mortality of 68.7% and a standard error of 3.8 (n = 8) compared to controls ($P < 0.0001$). Finally, we performed a nonparametric Wilcoxon pairwise analysis for 1-HP mortality between all of the strains, followed by a Benjamini−Hochberg Correction. We found that both the *ugt-23* and *ugt-49* mutants had significantly increased mortality compared to N2 ($P < 0.1$) (Figure 1B). This suggests that these genes play a role in the glycosylation of 1-HP. It is important to note that several factors might influence these results, most notably the genetic background of the mutation and the type or extent of the mutation. To examine these factors more closely in *ugt-23*, we generated a CRISPR *ugt-23* deletion (RB2550) through SUNY Biotech and compared this to the original *ugt-23* (PH7346) obtained through the CGC. There was a slight trend toward a higher percentage of death in the RB2550, but it was not statistically significant (P = 0.22, n = 6) (Supporting Information Figure 2C).

Isolation of Glycosylated 1-HP Derivatives. We then explored whether *ugt-23* and *ugt-49* produced the same 1-HP glycosylated products identified previously in N2.[12] We exposed larval stage 4 (L4) worms in large-scale liquid culture for 24 h, followed by high-performance liquid chromatography−ultraviolet (HPLC−UV) analysis of the worm media.

https://doi.org/10.1021/acs.chemrestox.3c00410
Chem. Res. Toxicol. 2024, 37, 590−599

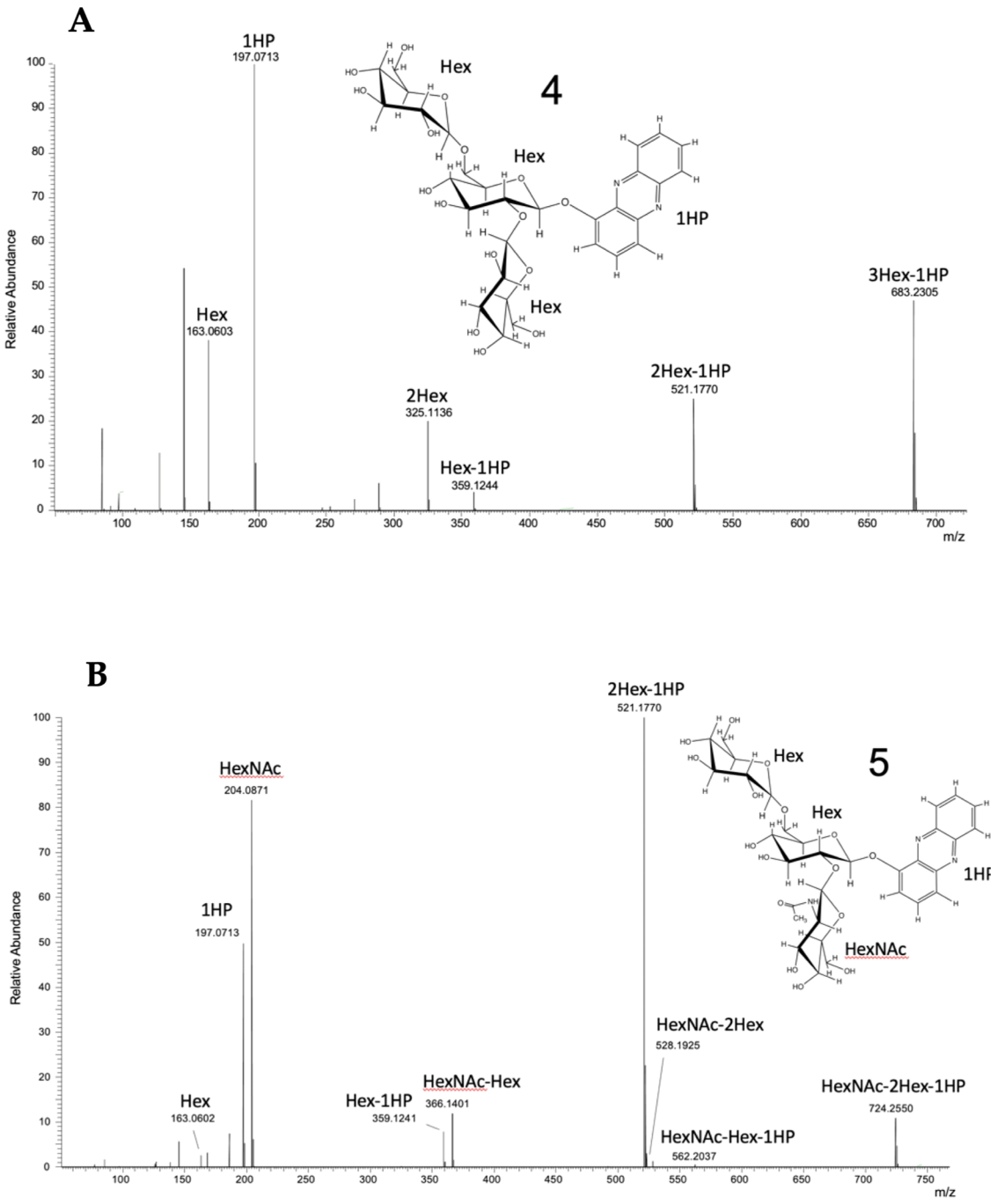

Figure 3. Tandem mass spectrometry (MS/MS) data for compounds (**4**) and (**5**). Tentative structural insets are based on NMR results discussed in detail below. (A) MS/MS Spectra for compound (**4**) with fragment ions corresponding to the loss of three hexose sugars. (B) MS/MS Spectra for compound (**5**) with fragment ions corresponding to the loss of two hexose and an *N*-acetyl hexose sugar.

We found that a 22.3 μM concentration allowed many worms to survive for 24 h to accumulate sufficient modified 1-HP. Using HPLC, we observed four unique peaks in all strains (Figure 2B). The peaks were isolated using semipreparative C-18 reverse phase HPLC and then analyzed by NMR and liquid chromatography−mass spectrometry (LC−MS)/MS (Figure 2A, Supporting Information Figures 3−7). We identified compounds (**2**) and (**3**), which had also been identified in prior literature (Figure 2A, Supporting Information Figures 3 and 4).[12] However, we also identified two branch-chained trisaccharides, one with three glucose moieties (**4**) and one with two glucose moieties and an *N*-acetylglucosamine (GlcNAc) (**5**) (Figure 2A).

Mass Spectrometry Analysis. Compounds (**4**) and (**5**) were obtained from fractionation of 1-HP derivatives. Molecular compositions were determined by accurate mass measurement, and tentative molecular structures were established using tandem mass spectrometry (MS/MS) (Figure 3A,B). The observed m/z of compound (**4**) was 683.2305 (theoretical value 683.2294, mass measurement error = 1.61 ppm) (Figure 2A, Supporting Information Table 2). The molecular formula was established as $C_{30}H_{38}N_2O_{16}$. The observed m/z of compound (**5**) was 724.255 [M + H^+]

https://doi.org/10.1021/acs.chemrestox.3c00410
Chem. Res. Toxicol. 2024, 37, 590−599

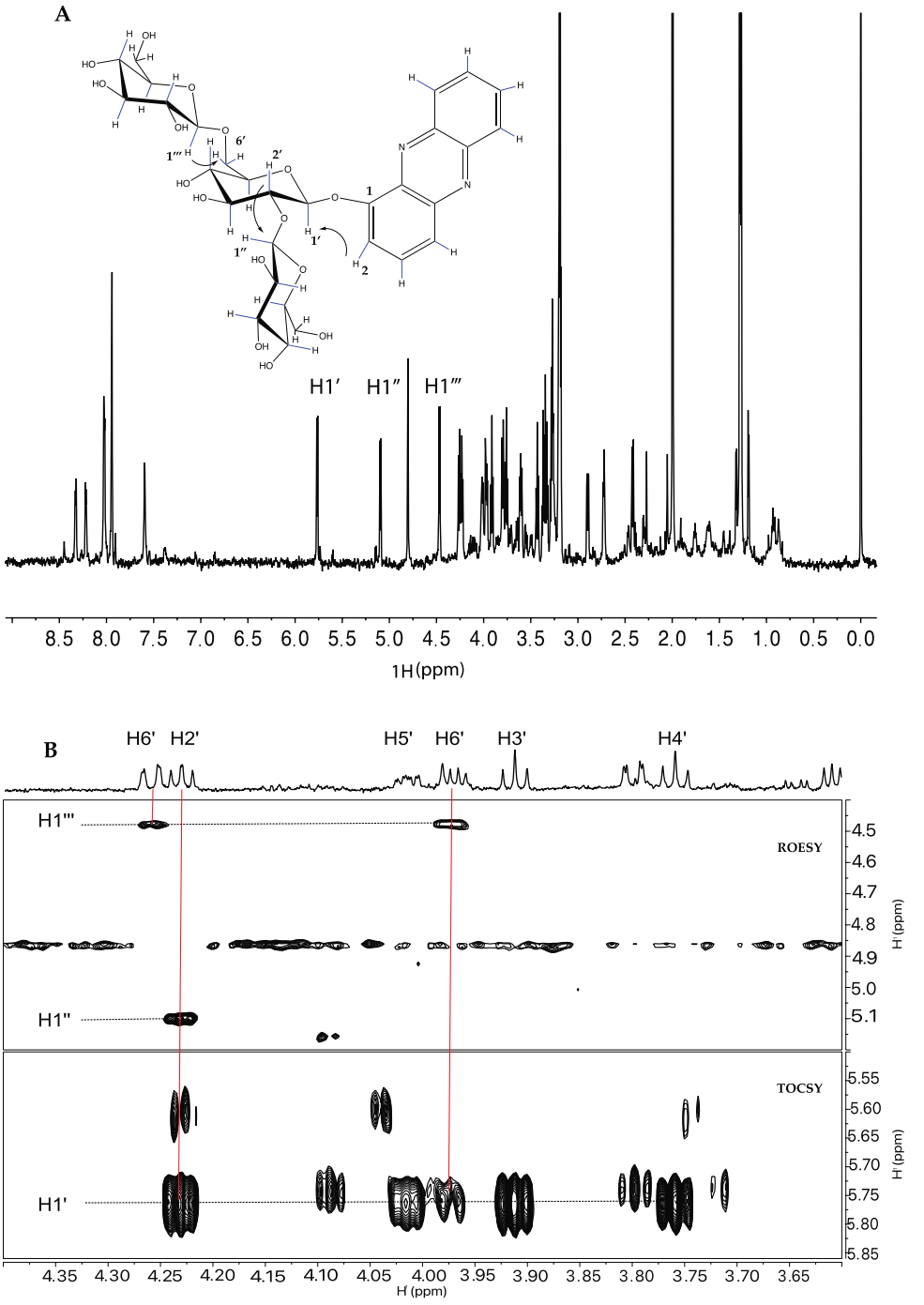

Figure 4. NMR spectra for trisaccharide compound (**4**): (A) Structure of compound (**4**) and 1D ^{1}H spectrum with β-glucosyl anomeric protons annotated. (B) Top panel shows a 1D ^{1}H of the glucosyl residue attached to the phenazine. The bottom panel is a region of a 2D TOCSY showing the protons coupled to H1′. The middle panel is a region of a 2D ROESY showing NOEs between H1″ and H1‴ and the respective protons in the linkage positions.

(theoretical value 724.2559), mass measurement error = 1.24 ppm (Figure 2A, Supporting Information Table 2), and the molecular formula was assigned as $C_{32}H_{41}N_3O_{16}$.

Higher-energy collisional dissociation (HCD) fragmentation of these compounds resulted in the generation of largely B-type glycosidic bond cleavages that enable the partial assignment of the molecular structure. MS/MS of compound (**4**) produced multiple fragment ions that support the modification of 1-HP by three hexose sugar units with the primary fragments annotated in Figure 3A. The sequential neutral loss of three hexose sugars due to glycosidic bond cleavage from the isolated molecular ion was observed, leading to a fragment identified as 1-HP (observed m/z 197.0713). Additional fragment ions corresponding to hexose units are also observed. The MS/MS of compound (**5**) produced multiple fragment ions, as shown in Figure 3B, which support the modification of 1-HP by two hexose sugars and one *N*-acetyl hexose sugar. Similar to the fragmentation observed in compound (**5**), the sequential neutral losses of sugar residues via glycosidic bond cleavage from the modified 1-HP

https://doi.org/10.1021/acs.chemrestox.3c00410
Chem. Res. Toxicol. 2024, 37, 590−599

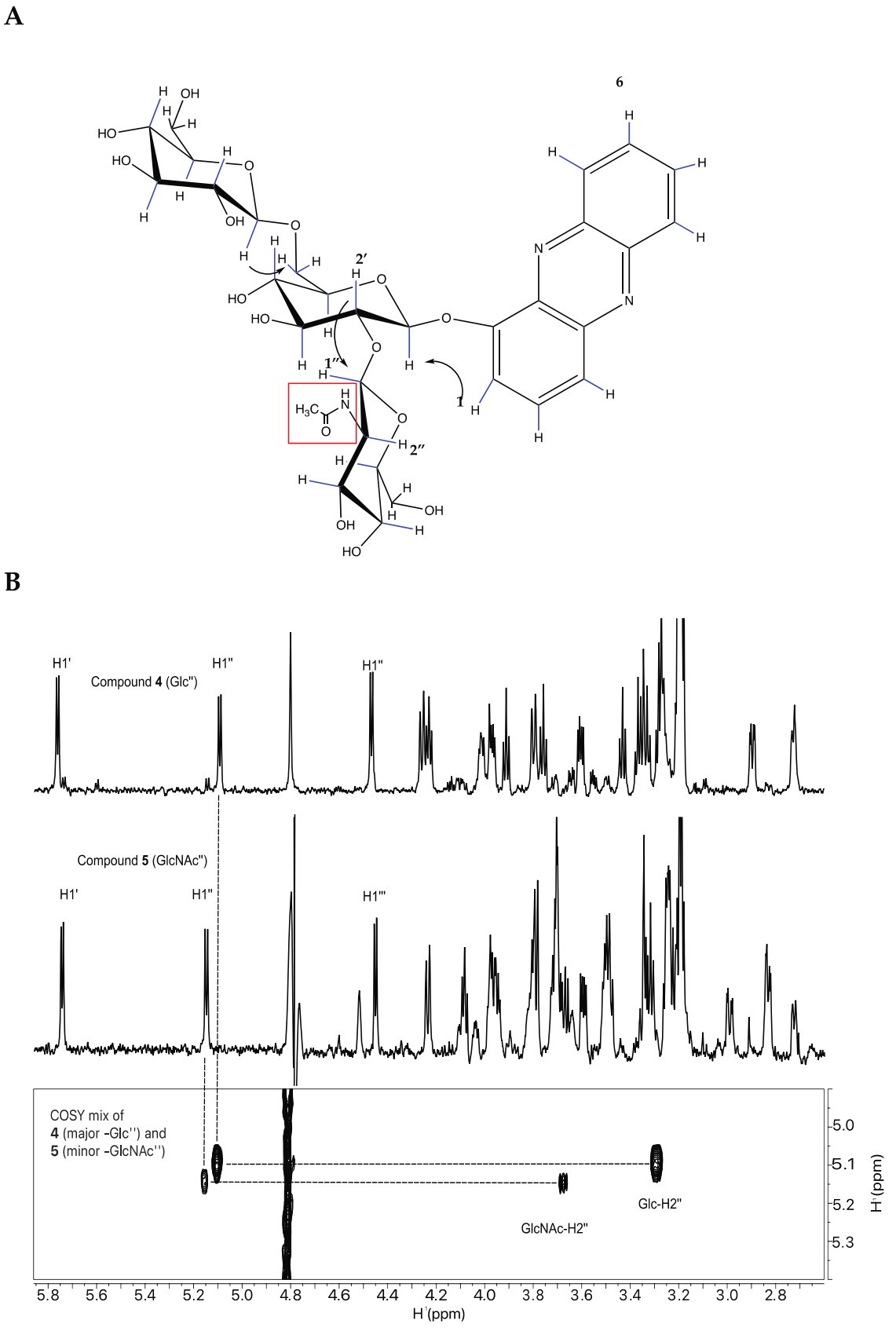

Figure 5. ^{1}H NMR spectrum supporting the *N*-acetyl-glucosamine containing compound (**5**): (A) Structure of compound **5**. (B) Middle panel shows the 1D proton of 5 and the three β-anomeric protons like those in compound (**4**) (top panel). The bottom panel is a region from a 2D COSY of the mixture of compound (**4**) (primary compound) and compound (**5**) (minor compound), indicating the chemical shift positions of H2″.

https://doi.org/10.1021/acs.chemrestox.3c00410
Chem. Res. Toxicol. 2024, 37, 590−599

molecular ion are also observed, with unique ions now present due to the inclusion of the *N*-acetyl moiety. A table of assigned fragments is provided as Supporting Information Table 3.

Nuclear Magnetic Resonance Analysis. The ^{1}H NMR spectrum of compound (**4**) (Figure 4A) contained signals corresponding to a phenazine and a sugar region with three anomeric protons, including two (H1′ and H1″) that are unusually downfield for β-anomers but consistent with being close to the aromatic phenazine. Analysis of data from 2D total correlation spectroscopy (TOCSY) and correlated spectroscopy (COSY) experiments (Supporting Information Figure 5.1) indicates that the three protons identified in the ^{1}H spectrum belong to three glucose moieties. The glucosyl attached to the phenazine and the glucosyl linked at C6 have chemical shifts very similar to those of the gentiobiose-phenazine described in Stupp et al.[12] The third glucosyl attached to C2 has very unusual shifts, consistent with the proximity to the phenazine, but the coupling patterns match the glucose configuration. Figure 4B illustrates the linkage position of compound (4), determined using 1D and 2D rotating frame Overhause effect spectroscopy (ROESY) data. The bottom panel shows a region from the TOCSY spectrum with H1′ along the horizontal at 5.77 ppm coupled to H2′−H6′; assignments are annotated in the top panel. This glucose is linked to the phenazine at the position shown in Figure 4A (see also Supporting Information Figure 5.2). The middle panel shows a region from the ROESY spectrum with a nuclear Overhauser effect (NOE) cross peak from H1″ at 5.1 ppm to H2′, establishing the H1″−H2 linkage. Similarly, the H1‴ proton at 4.47 ppm shows cross-peaks linking it to H6′ of the same phenazine-linked glucose.

The ^{1}H NMR spectrum of the minor compound (**5**) (Figure 5A) similarly displayed signals corresponding to phenazine and three sugar residues. However, a difference in chemical shift of H2″ (Figure 5B) suggested a β-*N*-acetyl-2-deoxy-glucosamine residue instead of a glucosyl residue (CASPER database),[24] consistent with the MS/MS data (Figure 3B). A combination of 1D and 2D TOCSY and 1D ROESY data (Supporting Information Figure 6) confirmed that the three residues were in the correct configuration, and the linkages were the same as in compound (**4**).

Because (**5**) contained a GlcNAc, we evaluated GlcNAc transferase mutant *ogt-1* with the same assays described above. *ogt-1* has previously been shown to modulate the immune response in *C. elegans* for *S. aureus* infection but not *P. aeruginosa* infection.[25] Consistent with those findings, the *ogt-1* knockout had no statistically significant difference in susceptibility to 1-HP compared with N2 and PD1074 (Figure 1B). LC−MS analysis of worm media conditioned by the *ogt-1* knockout mutant challenged with 1-HP showed that (**5**) was still produced (Supporting Information Figure 7).

Quantitation of 1-HP Derivatization in *ugt* Knockout Mutants. We then quantified the HPLC−UV data to observe if there was a reduction in the amounts of 1-HP derivatives for the *ugt-23* and *ugt-49* knockout mutants. We normalized the data to the sum of all of the 1-HP-related compounds for each replicate. This ensured that the ratio obtained was independent of any variation due to the amount of 1-HP the worms were exposed to or the number of worms per replicate. We found that the *ugt-23* knockout mutant produced decreased amounts of both trisaccharide sugars (**4**) and (**5**), while the *ugt-49* knockout mutant had reduced amounts of compounds (**3**), (**4**), and (**5**) (n = 7) (Figure 6).

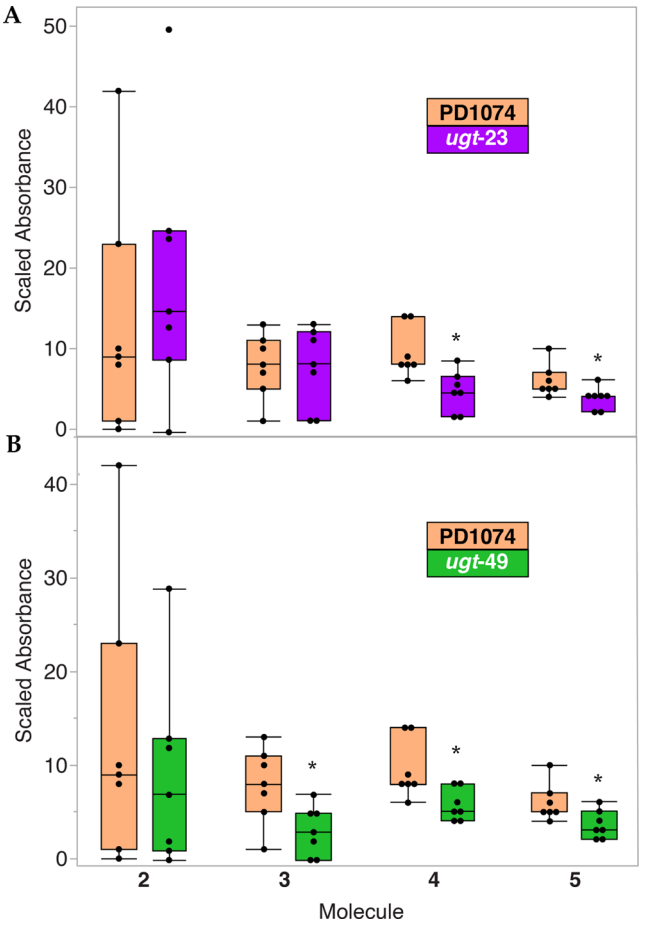

Figure 6. Box and whisker plot showing the relative amounts of 1-HP and its derivatives after a 24 h incubation at 22.3 μM 1-HP with 2% *E. coli* based on UV absorbance data. All replicates (n = 7) were paired, and data were normalized by dividing the absorbance for each compound at 260 nm by the sum of the absorbances of 1-HP and all its derivatives for each run (abs x/[abs z + abs y + abs x + abs w + abs v]). * Indicates a significant difference in relative amounts of compound compared to the relative amount of the same compound in PD1074 after Wilcoxon pairwise analysis (α = 0.05). (A) Relative amounts of glycosylated 1-HP derivatives for the *ugt-23* mutant compared to PD1074. Compounds **4** and **5** are reduced in this strain. (B) Relative amounts of glycosylated 1-HP derivatives for the *ugt-49* mutant compared to PD1074. Compounds **3**, **4**, and **5** are reduced in this strain.

These results show the involvement of *ugt* genes in 1-HP detoxification, suggesting that they have broad specificity and that multiple *ugt* genes are involved in detoxifying a xenobiotic in *C. elegans*. Prior research has implicated multiple *ugt* genes responsible for the glycosylation of other small-molecule toxins such as indole.[26] The workflow outlined in this study can be used to test the role of *ugt* genes in modifying other small-molecule xenobiotics. Future studies could validate whether broad specificity is seen in response to xenobiotics or whether this is a phenomenon specific to 1-HP.

Furthermore, our results implicate the addition of GlcNAc in detoxification in *C. elegans*, a result which, to our knowledge, was not previously observed. Our data also suggest that genes other than *ogt-1* are responsible for adding GlcNAc in the 1-HP glycosylation pathway. This might be due to the broad specificity of *ugt* genes or because GlcNAc serves a particular purpose in detoxification. Using this workflow, it would be

https://doi.org/10.1021/acs.chemrestox.3c00410
Chem. Res. Toxicol. 2024, 37, 590−599

interesting to see if GlcNAc-modified products are also observed for other xenobiotics.

METHODS

Mortality Assay. All 11 strains of *C. elegans* were grown and maintained on 10 cm nematode growth medium (NGM) agar plates seeded with a Luria−Bertani (LB)-cultured OP50 strain of *E. coli* at 22 °C. Knockout mutants were paired with an N2, and PD1074 replicates for each strain. 10 cm NGM plates with *C. elegans* were bleached and grown to L1 arrest, and then L1 arrested worms were transferred to new 10 cm plates and allowed to grow to L4. Upon reaching L4, ∼15 worms were assigned either to control 6 cm plates or 6 cm plates with NGM and 179 μM 1-HP, the LD_{50} value of PD1074.[22] Worms were incubated on experimental plates for 7 h. After 7 h, fluorescent beads were added to the worms, and the uptake of these beads was used as a marker to differentiate between live and dead worms.[27] We note that this method of scoring produces a nonzero background level of reported mortality (e.g., Supporting Information Figure 2) because worms that burrow into agar or crawl off the plate are scored as dead.

Lifespan Timing Assay. Worms were observed to determine how long they took to go from the egg to L4 in two different ways. The time to L4 for N2, PD1074, and the *ugt-1*, *ugt-23*, *ugt-49*, *ugt-60*, and *ugt-62* knockout mutants was measured by initially spot bleaching a single adult and following a single egg, observing them until they reached L4. The time to L4 for the *ugt-6*, *ugt-9*, *ugt-66*, and *ogt-1* knockout mutants was measured by bleach synchronization of a plate of worms and placing the resulting eggs on a 10 cm plate. The plates were observed every 4−8 h until most of the population on the plate could reliably be identified as L4.

Large-Scale Growth of *C. elegans*. Worms were grown on large-scale culture plates (LSCPs) to generate worms for subsequent experiments. LSCPs were poured according to previously described protocols.[28] LSCPs are hand-washed, sterilized, and wiped with 70% ethanol. The nematode growth medium (NGM) was prepared as a mixture of MYOB, agarose, and bacto-peptone in a ratio of 5.9:10:10 g L^{-1}. Poured plates were seeded with the HTS115 strain of *E. coli* prepared in K-media at a concentration of 0.5 g mL^{-1} bacteria generated according to the IBAT method.[29] Worms were chunked onto the LSCPs and then grown for 7−10 days, depending on the strain, before being washed with M9 for subsequent experiments. After washing, worms were bleach synchronized and then grown to L1 arrest in M9. Upon reaching L1 arrest, they were transferred to an S-basal medium (∼30,000 worms mL^{-1}) and incubated with 2% *E. coli* OP50 until they reached L4. After the worms had reached L4, they were incubated with either 1.1% DMSO or 22.3 μM 1-HP. Worms were incubated for 24 h and then centrifuged. The supernatant was collected for subsequent experiments.

Glucoside Collection and Analysis (HPLC−UV). After the supernatant was separated from the worms, it was centrifuged again at 20,800 relative centrifugal force (RCF) for 10 min to separate the bacteria from the supernatant. The resultant volume was lyophilized and extracted in an appropriate volume of methanol (200 and 600 μL, depending on the starting volume of the supernatant). It was then centrifuged at 20,800 RCF for 30 min. Following centrifugation, the supernatant was concentrated to ∼100 μL with 90 μL injected into HPLC−UV and 10 μL separated for LC−MS.

The supernatant was analyzed on an Agilent 1200 Series HPLC system with a diode array collector, and fractions were collected manually upon observation of a peak. Absorbance was measured at 260 nm. For worm media separation, 5% methanol (A) and 95% 5 mM phosphate buffer pH 7.2 (B) were held isocratic for 4 min, increasing to 95% A and 5% B over 30 min, and then held for 5 min, followed by a re-equilibration of the column. The separation was carried out at a flow rate of 2 mL min^{-1} in an Agilent SB C-18 column (9.4 mm × 250 mm, 5 μM).

After initial fractionation, further separation of the fraction containing compounds **4** and **5** was carried out. For that separation, 5% methanol (A) and 95% five mM phosphate buffer pH 7.2 (B) were held isocratic for 4 min, increasing to 50% A and 50% B over 17 min. The gradient was slowed, and the ratio was increased to 67% A and 33% B by 28 min before ramping it up to 95% A and 5% B by 30 min and then holding constant for 5 min. A re-equilibration of the column followed this. The column used for this separation was the same as that for the initial worm media separation.

Glucoside Analysis (LC−MS/MS). Samples aliquoted during glucoside collection were analyzed using a Thermo Fisher Scientific Q Exactive HF Orbitrap mass spectrometer coupled to a Vanquish UPLC instrument with inline UV detection. Chromatographic separation was performed with an Agilent ZORBAX Eclipse XDB-C-18 column (2.1 mm × 150 mm, 1.8 μm) over 30 min, starting with 95% H_2O (A) and 5% methanol (B) held isocratic for 2.5 min, then increased to 70% B by 22 min and 100% B at 22.5 min, and held for 4 min before re-equilibration at 5% B for 3 min prior the next injection. The sample queue was randomized with injection blanks included to monitor for sample carryover. All samples were analyzed by positive mode electrospray ionization (ESI). Full MS scans were performed at a specified resolution of 30,000 (m/z 200) from 150 to 2000 m/z with an AGC target of 3e6 and a maximum IT of 200 ms. Corresponding UV traces were collected at 260 nm.

Target compounds were isolated with a 4.0 m/z quadrupole window to perform structural elucidation by higher-energy collisional dissociation (HCD). A normalized collision energy (NCE) of 15 V was applied, and fragment ions were detected with a specified resolution of 15,000, AGC target of 2e5, and a maximum of IT 100 ms. MS data were analyzed with the Thermo Qual Browser and manually interpreted.

Glucoside Analysis (NMR). Pooled fractions were dried, resuspended in 60 μL of D_2O with 0.15 mM DSS as an internal standard, dried with a speed vac, and resuspended twice in 60 μL of D_2O to perform buffer exchange to remove excess H_2O before being transferred into 1.7 mm NMR tubes. 1D ^1H, 2D COSY, 2D TOCSY, selective 1D TOCSY, and selective 1D ROESY spectra were collected where appropriate on a Bruker 800 MHz NEO spectrometer using a 1.7 mm cryoprobe. Spectra were processed and analyzed with MestReNova 14.1.2 (Mestrelab Research).

Statistical Analysis. Analysis was performed using JMP, a publicly available statistical software. A Wilcoxon test, followed by a Wilcoxon pairwise analysis and a Benjamini−Hochberg correction, was performed for the mortality assays to determine the significance between strains. Tukey's HSD test was performed to determine the significance within each strain for 1-HP exposure. A Wilcoxon test followed by Wilcoxon pairwise analysis was performed on the scaled absorbance data.

ASSOCIATED CONTENT

Supporting Information

The Supporting Information is available free of charge at https://pubs.acs.org/doi/10.1021/acs.chemrestox.3c00410.

> Detailed strain information; high-resolution MS data for 1-HP derived metabolites; associated MS/MS data; a phylogenetic tree explaining the relationship between the different members of the UGT family in *C. elegans*; detailed mortality data; and supporting NMR, MS, and MS/MS data (PDF)

AUTHOR INFORMATION

Corresponding Author

Arthur S. Edison − *Department of Biochemistry & Molecular Biology, University of Georgia, Athens, Georgia 30602, United States; Complex Carbohydrate Research Center and Institute of Bioinformatics, University of Georgia, Athens, Georgia 30602, United States;* orcid.org/0000-0002-5686-2350; Email: aedison@uga.edu

https://doi.org/10.1021/acs.chemrestox.3c00410
Chem. Res. Toxicol. 2024, 37, 590−599

Authors

Muhammad Zaka Asif − *Department of Biochemistry & Molecular Biology, University of Georgia, Athens, Georgia 30602, United States; Complex Carbohydrate Research Center, University of Georgia, Athens, Georgia 30602, United States;* Present Address: Florida Atlantic University, 5353 Parkside Dr., Jupiter, Florida 33458, United States

Kelsey A. Nocilla − *Complex Carbohydrate Research Center, University of Georgia, Athens, Georgia 30602, United States;* orcid.org/0000-0002-6759-9391

Li Ngo − *Complex Carbohydrate Research Center, University of Georgia, Athens, Georgia 30602, United States*

Man Shah − *Complex Carbohydrate Research Center, University of Georgia, Athens, Georgia 30602, United States*

Yosef Smadi − *Complex Carbohydrate Research Center, University of Georgia, Athens, Georgia 30602, United States*

Zaki Hafeez − *Complex Carbohydrate Research Center, University of Georgia, Athens, Georgia 30602, United States*

Michael Parnes − *Complex Carbohydrate Research Center, University of Georgia, Athens, Georgia 30602, United States*

Allie Manson − *Complex Carbohydrate Research Center, University of Georgia, Athens, Georgia 30602, United States*

John N. Glushka − *Complex Carbohydrate Research Center, University of Georgia, Athens, Georgia 30602, United States*

Franklin E. Leach, III − *Complex Carbohydrate Research Center and Department of Chemistry, University of Georgia, Athens, Georgia 30602, United States;* orcid.org/0000-0002-3292-1096

Complete contact information is available at: https://pubs.acs.org/10.1021/acs.chemrestox.3c00410

Notes

The authors declare no competing financial interest.

■ ACKNOWLEDGMENTS

The authors thank Olatomiwa Bifarin (Georgia Tech) for helpful discussions on designing worm toxicity experiments. The authors thank Gonçalo Gouveia (Cornell University), Amanda Shaver (Northwestern University), and Pam Kirby (University of Georgia) for help and discussions on large-scale worm growth protocols. The authors thank Laura Morris and Ricardo Borges (University of Georgia) for their help with using the HPLC instrument and for valuable data analysis discussions. The TOC worm image was created using BioRender. This work was supported by NIH 1U2CES030167, NIH 5R35GM148240-02, and the Georgia Research Alliance.

■ REFERENCES

(1) (a) Barriere, A.; Felix, M. A. Isolation of C. elegans and related nematodes. *WormBook* **2006**, 1−9. (b) Frézal, L.; Felix, M. A. C. elegans outside the Petri dish. *eLife* **2015**, *4*, No. e.05849, DOI: 10.7554/eLife.05849.

(2) Schulenburg, H.; Felix, M. A. The Natural Biotic Environment of Caenorhabditis elegans. *Genetics* **2017**, *206* (1), 55−86.

(3) (a) Pradel, E.; Zhang, Y.; Pujol, N.; Matsuyama, T.; Bargmann, C. I.; Ewbank, J. J. Detection and avoidance of a natural product from the pathogenic bacterium Serratia marcescens by Caenorhabditis elegans. *Proc. Natl. Acad. Sci. U.S.A.* **2007**, *104* (7), 2295−2300. (b) Schulenburg, H.; Ewbank, J. J. The genetics of pathogen avoidance in Caenorhabditis elegans. *Mol. Microbiol.* **2007**, *66* (3), 563−570.

(4) Engelmann, I.; Pujol, N. Innate immunity in C. elegans. *Adv. Exp. Med. Biol.* **2010**, *708*, 105−121.

(5) Stasiuk, S. J.; MacNevin, G.; Workentine, M. L.; Gray, D.; Redman, E.; Bartley, D.; Morrison, A.; Sharma, N.; Colwell, D.; Ro, D. K.; Gilleard, J. Similarities and differences in the biotransformation and transcriptomic responses of Caenorhabditis elegans and Haemonchus contortus to five different benzimidazole drugs. *Int. J. Parasitol.: Drugs Drug Resist.* **2019**, *11*, 13−29.

(6) Williams, R. T. *Detoxification Mechanisms: The Metabolism and Detoxification of Drugs, Toxic Substances and Other Organic Compounds*; Chapman & Hall: London, 1959.

(7) Hartman, J. H.; Widmayer, S. J.; Bergemann, C. M.; King, D. E.; Morton, K. S.; Romersi, R. F.; Jameson, L. E.; Leung, M. C. K.; Andersen, E. C.; Taubert, S.; Meyer, J. N. Xenobiotic metabolism and transport in Caenorhabditis elegans. *J. Toxicol. Environ. Health, Part B* **2021**, *24* (2), 51−94.

(8) (a) Prabhu, M. S.; Walawalkar, Y. D.; Furtado, I. Purification and molecular and biological characterisation of the 1-hydroxyphenazine, produced by an environmental strain of Pseudomonas aeruginosa. *World J. Microbiol. Biotechnol.* **2014**, *30* (12), 3091−3099. (b) Qi, X. Z.; Xue, M. Y.; Cui, H. B.; Yang, K. C.; Song, K. G.; Zha, J. W.; Wang, G. X.; Ling, F. Antimicrobial activity of Pseudomonas monteilii JK-1 isolated from fish gut and its major metabolite, 1-hydroxyphenazine, against Aeromonas hydrophila. *Aquaculture* **2020**, *526*, No. 735366. (c) Wan, Y.; Liu, H.; Xian, M.; Huang, W. Biosynthesis and metabolic engineering of 1-hydroxyphenazine in Pseudomonas chlororaphis H18. *Microb. Cell Fact.* **2021**, *20* (1), No. 235. (d) Watson, D.; MacDermot, J.; Wilson, R.; Cole, P. J.; Taylor, G. W. Purification and structural analysis of pyocyanin and 1-hydroxyphenazine. *Eur. J. Biochem.* **1986**, *159* (2), 309−313.

(9) Wilson, R.; Pitt, T.; Taylor, G.; Watson, D.; MacDermot, J.; Sykes, D.; Roberts, D.; Cole, P. Pyocyanin and 1-hydroxyphenazine produced by Pseudomonas aeruginosa inhibit the beating of human respiratory cilia in vitro. *J. Clin. Invest.* **1987**, *79* (1), 221−229.

(10) Cezairliyan, B.; Vinayavekhin, N.; Grenfell-Lee, D.; Yuen, G. J.; Saghatelian, A.; Ausubel, F. M. Identification of Pseudomonas aeruginosa Phenazines that Kill Caenorhabditis elegans. *PLoS Pathog.* **2013**, *9* (1), No. e1003101.

(11) Ray, A.; Rentas, C.; Caldwell, G. A.; Caldwell, K. A. Phenazine derivatives cause proteotoxicity and stress in C. elegans. *Neurosci. Lett.* **2015**, *584*, 23−27.

(12) Stupp, G. S.; von Reuss, S. H.; Izrayelit, Y.; Ajredini, R.; Schroeder, F. C.; Edison, A. S. Chemical Detoxification of Small Molecules by Caenorhabditis elegans. *ACS Chem. Biol.* **2013**, *8* (2), 309−313.

(13) (a) Audet-Delage, Y.; Rouleau, M.; Villeneuve, L.; Guillemette, C. The Glycosyltransferase Pathway: An Integrated Analysis of the Cell Metabolome. *Metabolites* **2022**, *12* (10), No. 1006, DOI: 10.3390/metabo12101006. (b) Lindblom, T. H.; Dodd, A. K. Xenobiotic detoxification in the nematode Caenorhabditis elegans. *J. Exp. Zool., Part A* **2006**, *305a* (9), 720−729.

(14) Hu, D. G.; Mackenzie, P. I.; Hulin, J. A.; McKinnon, R. A.; Meech, R. Regulation of human UDP-glycosyltransferase (UGT) genes by miRNAs. *Drug Metab. Rev.* **2022**, *54* (2), 120−140.

(15) Asif, M. Z.; Benveniste, M. C.; Chism, K. D.; Levin, A. L.; Lanier, D.; Watkins, R. E.; Taujale, R.; Tucker, N.; Edison, A. S. Computational analysis of variation in C. elegans ugts. *MicroPubl. Biol.* **2023**, *2023*, 1 DOI: 10.17912/micropub.biology.000819.

(16) Fontaine, P.; Choe, K. The transcription factor SKN-1 and detoxification gene ugt-22 alter albendazole efficacy in Caenorhabditis elegans. *Int. J. Parasitol.: Drugs Drug Resist.* **2018**, *8* (2), 312−319.

(17) Cui, Y. X.; McBride, S. J.; Boyd, W. A.; Alper, S.; Freedman, J. H. Toxicogenomic analysis of Caenorhabditis elegans reveals novel genes and pathways involved in the resistance to cadmium toxicity. *Genome Biol.* **2007**, *8* (6), No. R122, DOI: 10.1186/gb-2007-8-6-r122.

(18) (a) Di, R.; Zhang, H. Z.; Lawton, M. A. Transcriptome Analysis of C. elegans Reveals Novel Targets for DON Cytotoxicity. *Toxins* **2018**, *10* (7), No. 262, DOI: 10.3390/toxins10070262. (b) Hasegawa, K.; Miwa, S.; Isomura, K.; Tsutsumiuchi, K.; Taniguchi, H.; Miwa, J. Acrylamide-responsive genes in the nematode Caenorhabditis elegans.

Toxicol. Sci. **2008**, *101* (2), 215−225. (c) Hasegawa, K.; Miwa, S.; Tsutsumiuchi, K.; Miwa, J. Allyl Isothiocyanate that Induces GST and UGT Expression Confers Oxidative Stress Resistance on C. elegans, as Demonstrated by Nematode Biosensor. *PLoS One* **2010**, *5* (2), No. e9267. (d) Laing, S. T.; Ivens, A.; Laing, R.; Ravikumar, S.; Butler, V.; Woods, D. J.; Gilleard, J. S. Characterization of the xenobiotic response of Caenorhabditis elegans to the anthelmintic drug albendazole and the identification of novel drug glucoside metabolites. *Biochem. J.* **2010**, *432*, 505−514. (e) Taubert, S.; Hansen, M.; Van Gilst, M. R.; Cooper, S. B.; Yamamoto, K. R. The mediator subunit MDT-15 confers metabolic adaptation to ingested material. *PLoS Genet.* **2008**, *4* (2), No. e1000021.

(19) Brenner, S. The genetics of Caenorhabditis elegans. *Genetics* **1974**, *77* (1), 71−94.

(20) Cook, D. E.; Zdraljevic, S.; Roberts, J. P.; Andersen, E. C. CeNDR, the Caenorhabditis elegans natural diversity resource. *Nucleic Acids Res.* **2017**, *45* (D1), D650−D657.

(21) Yoshimura, J.; Ichikawa, K.; Shoura, M. J.; Artiles, K. L.; Gabdank, I.; Wahba, L.; Smith, C. L.; Edgley, M. L.; Rougvie, A. E.; Fire, A. Z.; et al. Recompleting the Caenorhabditis elegans genome. *Genome Res.* **2019**, *29* (6), 1009−1022.

(22) Au, V.; Li-Leger, E.; Raymant, G.; Flibotte, S.; Chen, G.; Martin, K.; Fernando, L.; Doell, C.; Rosell, F. I.; Wang, S.; et al. CRISPR/Cas9 Methodology for the Generation of Knockout Deletions in Caenorhabditis elegans. *G3 (Bethesda)* **2019**, *9* (1), 135−144.

(23) Asif, M. Z.; Van der Gaag, V. L.; Guo, J.; Nocilla, K. A.; Muzio, C. J.; Edison, A. S. A Plate Based Assay for Determination of the Median Lethal Dose of 1-Hydroxyphenazine in Caenorhabditis elegans. *MicroPubl. Biol.* **2021**, *2021*, 1 DOI: 10.17912/micropub.biology.000352.

(24) Furevi, A.; Ruda, A.; Angles d'Ortoli, T.; Mobarak, H.; Ståhle, J.; Hamark, C.; Fontana, C.; Engström, O.; Apostolica, P.; Widmalm, G. Complete 1H and 13C NMR chemical shift assignments of mono- to tetrasaccharides as basis for NMR chemical shift predictions of oligo- and polysaccharides using the computer program CASPER. *Carbohydr. Res.* **2022**, *513*, No. 108528, DOI: 10.1016/j.carres.2022.108528.

(25) Bond, M. R.; Ghosh, S. K.; Wang, P.; Hanover, J. A. Conserved Nutrient Sensor O-GlcNAc Transferase Is Integral to C. elegans Pathogen-Specific Immunity. *PLoS One* **2014**, *9* (12), No. e113231.

(26) Lee, J. H.; Kim, Y. G.; Kim, M.; Kim, E.; Choi, H.; Kim, Y.; Lee, J. Indole-associated predator-prey interactions between the nematode Caenorhabditis elegans and bacteria. *Environ. Microbiol.* **2017**, *19* (5), 1776−1790.

(27) Kiyama, Y.; Miyahara, K.; Ohshima, Y. Active uptake of artificial particles in the nematode Caenorhabditis elegans. *J. Exp. Biol.* **2012**, *215* (Pt 7), 1178−1183.

(28) Shaver, A. O.; Gouveia, G. J.; Kirby, P. S.; Andersen, E. C.; Edison, A. S. Culture and Assay of Large-Scale Mixed-Stage Caenorhabditis elegans Populations. *J. Visualized Exp.* **2021**, No. 171, No. e61453.

(29) Gouveia, G. J.; Shaver, A. O.; Garcia, B. M.; Morse, A. M.; Andersen, E. C.; Edison, A. S.; McIntyre, L. M. Long-Term Metabolomics Reference Material. *Anal. Chem.* **2021**, *93* (26), 9193−9199.

https://doi.org/10.1021/acs.chemrestox.3c00410
Chem. Res. Toxicol. 2024, 37, 590−599